Analytical and Bioanalytical Chemistry (2019) 411:6265–6274
https://doi.org/10.1007/s00216-019-02021-8

PAPER IN FOREFRONT

Fundamental study of ion trapping and multiplexing using drift tube-ion mobility time-of-flight mass spectrometry for non-targeted metabolomics

Tim J. Causon[1] · Le Si-Hung[1] · Kenneth Newton[2] · Ruwan T. Kurulugama[2] · John Fjeldsted[2] · Stephan Hann[1]

Received: 9 May 2019 / Revised: 21 June 2019 / Accepted: 4 July 2019 / Published online: 13 July 2019

Abstract

This study of ion accumulation/release behavior relevant to ion mobility–mass spectrometry (IM-MS) as employed for non-targeted metabolomics involves insight from theoretical studies, and controlled reference experiments involving measurement of low and high molecular mass metabolites in varying concentrations within a complex matrix (yeast extracts). Instrumental settings influencing ion trapping (accumulation time) and release conditions in standard and multiplexed operation have been examined, and translation of these insights to liquid chromatography (LC) in combination with drift tube IM-MS measurements has been made. The focus of the application is non-targeted metabolomics using carefully selected samples to allow quantitative interpretations to be made. Experimental investigation of the IM-MS ion utilization efficiency particularly focusing on the use of the Hadamard transform multiplexing with 4-bit pseudo-random pulsing sequence for assessment of low and high molecular mass metabolites is compared with theoretical modeling of gas-phase behavior of small and large molecules in the IM trapping funnel. Increasing the trapping time for small metabolites with standard IM-MS operation is demonstrated to have a deleterious effect on maintaining a quantitative representation of the metabolite abundance. The application of these insights to real-world non-targeted metabolomics assessment of intracellular extracts from biotechnologically relevant production processes is presented, and the results were compared to LC×IM-MS measurements of the same samples. Spiking of a uniformly ^{13}C-labeled yeast extract (as a standard matrix) with varying amounts of natural metabolites is used to assess the linearity and sensitivity according to the instrument mode of operation (i.e., LC-MS, LC×IM-MS, and LC×[multiplexed]IM-MS). When comparing metabolite quantification using standard and multiplexed operation, sensitivity gain factors of 2–8 were obtained for metabolites with m/z below 250. Taken together, the simulation and experimental results of this study provide insight for optimizing measurement conditions for metabolomics and highlight the need for implementation of multiplexing strategies using short trapping times as relative quantification (e.g., in the context with non-targeted differential analysis) with sufficient sensitivity and working range is a requirement in this field of application.

Keywords *CCS* · Hadamard · Ion mobility · Liquid chromatography · Mass spectrometry · Metabolomics · Multiplexing · Yeast

Introduction

Liquid chromatography with drift-tube ion mobility time-of-flight mass spectrometry (LC×DTIM-TOFMS) is now a powerful platform for metabolomics [1–5]. Recent contributions toward the standardization of measurement conditions to a traceable reference has allowed collision cross sections derived from DTIM-MS measurements (^{DT}CCS) to be used as an accurate molecular identifier [6]. Several experimental studies have already utilized DTIM-MS as well as secondary IM-MS platforms for non-targeted metabolomics studies using LC and solid-phase extraction (SPE) platforms [7–13]. Within these studies, the instrumentation used allows the

Published in the topical collection *Close-Up of Current Developments in Ion Mobility Spectrometry* with guest editor Gérard Hopfgartner.

Electronic supplementary material The online version of this article (https://doi.org/10.1007/s00216-019-02021-8) contains supplementary material, which is available to authorized users.

✉ Tim J. Causon
tim.causon@boku.ac.at

[1] Institute of Analytical Chemistry, Department of Chemistry, University of Natural Resources and Life Sciences, Vienna (BOKU), Muthgasse 18, 1190 Vienna, Austria

[2] Agilent Technologies, Santa Clara, CA 95051, USA

mobility-based separation of all ionized species (i.e., a generic IM technique), which is a critical requirement for generating data suitable for non-targeted metabolomics investigations.

In terms of the type of experimental questions addressed within metabolomics studies, differential strategies are often used to identify metabolite-level changes related to specific conditions, e.g., pinpointing previously unknown metabolic rearrangements, biomarker discovery, influence of growth media, exposure, or assessment of genetic variants [14, 15]. While not able to provide coverage of all metabolites in a single run, LC or 2DLC in combination with high-resolution MS continues to be a primary platform for such studies as it represents an acceptable compromise in terms of coverage with respect to analysis time [16]. From a bottom-up perspective, generation of datasets suitable for non-targeted metabolomics therefore requires software-based binning of single molecular species according to chromatographic alignment and chemical relations such as expected isotopologue ratios, spacing, and appearance of related ion species including dimers and adducts. Following this assessment, the total abundance of a putative metabolite is determined as an integrated signal corresponding to this preliminary assessment and is used as proxy for the amount present in the sample. When considering use of LC×IM-TOFMS, all of these considerations and steps are retained within a general workflow, but also require alignment according to determined arrival time of the IM peak (often referred to as "drift time"), or a *CCS* value derived by a suitable calibration strategy. Thus, in seeking to add the mobility-derived *CCS* as an additional identification point for metabolomics workflows, detailed investigation of repeatability, generation of signal artifacts, and assessment of analytical figures of merit are considered critical for endorsement and finally comprehensive validation of analytical methods developed on such platforms. As such, use of LC×IM-TOFMS retains these steps used in this general non-targeted metabolomics approach and should be critically addressed as such platforms become more frequently used.

As a first key instrumental and acquisition point of difference, use of an IM separation between LC and TOF MS while retaining a suitable duty cycle necessitates use of transient ion trapping/accumulation and release events [17]. While most IM multiplexing approaches such as the Fourier and Hadamard transform allow improvements in the duty cycle in comparison with standard operation ion gating or pulsing approaches (i.e., one ion packet per IM cycle), the practical limitations for metabolomics studies necessitate the use of extended uniform trapping times to provide comparable numbers of ions reaching the mass detector (referred to as "ion utilization efficiency" [18]) and allow for more reliable relative quantification across different samples (i.e., differential analysis). The commercially available instrument used in the present study has capabilities to perform Hadamard multiplexing experiments with 3-bit and 4-bit simplex matrix-based pseudo-random sequence (PRS) pulsing, whereby the same uniform trapping time is used for each "1" in the PRS. However, it is postulated that these trapping events can lead to space-charge effects and subsequent changes in the ion population distribution [19]. As a key requirement of metabolomics workflows is that a quantitative snapshot of the metabolome be provided by the analysis, the nature of ion accumulation/trapping processes and their impact on differential metabolome assessment remains a point requiring both fundamental and application-based investigations.

Development of non-targeted workflows using LC in combination with a commercially available IM-TOFMS instrument requires optimization of multiple acquisition parameters in accordance with expected analytical method validation protocols. In this study, we have thus investigated the key trapping parameters necessary for LC×IM-TOFMS operation within the context of an exemplary non-targeted metabolomics workflow with particular focus on the suitability and potential benefits of using multiplexed operation.

Experimental

Chemicals

LC-MS-grade methanol, water, ammonium formate, and formic acid were purchased from Sigma-Aldrich. A total of 36 metabolite standards covering a mass range of 90–788 *m/z* was prepared with target concentrations of 5 or 10 mmol/L using suitable additives (0.1 mol/L HCl, 0.1% v/v formic acid, 0.1 mol/L NaOH) as necessary (see Electronic Supplementary Material (ESM) Table S1). Certified reference material for amino acids in 0.1 mol/L hydrochloric acid (NIST 2389a) was purchased from NIST. The reference mixture of tune ions used for instrument tuning, *m/z* calibration, and single-field ^{DT}CCS calibration was prepared according to the manufacturer's instructions for this instrument class and ion source.

Preparation of samples, reference material, and quality control protocols

For assessment of trueness, certified reference material and corresponding external calibration solutions prepared from solid metabolite standards were prepared by dilution in 0.1% v/v formic acid in the concentration range of 1–100 μmol/L.

For assessments representing conventional non-targeted metabolomics workflows, a $U^{13}C$-labeled internal standard ($U^{13}C$ ISTD) mixture prepared from *Pichia pastoris* (a methylotrophic yeast) was obtained from ISOtopic Solutions (Vienna, Austria). The *P. pastoris* sample contains dry extract of more than 2×10^9 cells (approximately 15 mg cell dry weight) and represents a full set of high-purity $U^{13}C$-labeled internal standards used for metabolomics studies. The $U^{13}C$

ISTD was spiked with different concentration levels of a 100-μmol/L mixture of the 36 natural metabolites to facilitate internal calibration experiments (0–30 μmol/L) and non-targeted screening of natural metabolites in a complex, but non-interfering matrix with respect to the metabolites present. An additional quality control (QC) sample comprising only the 36 natural metabolites in an aqueous solution with a concentration of 10 μmol/L was also prepared.

Following initial instrument equilibration and measurement of solvent blanks, the analytical sequence followed concentration order (0, 0.3, 1.0, 3.0, 10, 30 μmol/L) followed by a QC injection and an additional unspiked sample (i.e., 0 μmol/L) for each respective method. The total sequence time was approximately 25 h covering an internal calibration using analogous methods referred to as LC×TOFMS, LC×IM-TOFMS, and LC×IM-TOFMS with 4-bit multiplexing (LC×^{4}mIM-TOFMS). Data were collected for each method in triplicate with blocked alternation between methods used to avoid instrument drift affecting results (see ESM Table S5).

HPLC-MS instrumentation

For all measurements, an Agilent 1290 Infinity II LC system coupled to an Agilent 6560 IM-QTOF mass spectrometer with an Agilent dual Jetstream ESI source and electronic drift gas pressure control module was used. A solution containing calibrant ions (purine and hexakis-(1H,1H,3H-tetrafluoropentoxy) phosphazene) was mixed using a T-piece with the effluent using an additional HPLC pump (Agilent 1100 series) operated with a flow rate of 10 μL/min. It is noted that the secondary sprayer of the ESI source was closed to gas and liquid flow. All injections of sample injection (loop size of 5 μL) were carried out using a GERSTEL Dual Rail MPS 2 robot (Mülheim an der Ruhr, Germany).

LC×IM-TOFMS and heart-cut 2DLC×IM-TOFMS conditions

The primary chromatographic methods were adapted from previous work [20]. Briefly, a silica-based Atlantis T3 C18 column (2.1 × 150 mm, 3 μm d_p, Waters) was used for reversed-phase (RP) separations with a flow rate of 250 μL/min. Mobile phase A was water with 0.1% v/v formic acid and 1% v/v acetonitrile; mobile phase B was acetonitrile with 0.1% v/v formic acid and 1% v/v water. A gradient from 0 to 95% B in 13 min was used following a 2-min isocratic step. Including a cleaning step at 95% B and column re-equilibration at initial gradient conditions, the total run time was 20 min. For heart-cut experiments, the second column was a porous graphitized carbon Hypercarb column (2.1 × 150 mm, 5 μm d_p, Thermo Scientific) with a flow rate of 250 μL/min. Mobile phase A was water with 1% acetonitrile. Mobile phase B contained 90% water and 10% formic acid. A gradient from 1 to 40% B in 11.5 min was used following a 2.5-min isocratic operation. Including a cleaning step at 40% B and column re-equilibration at initial gradient conditions, the total run time was 20 min. The injection volume was 5 μL and a column oven temperature was set to 45 °C unless otherwise indicated. The heart-cut transfer of the initial fraction from the first-dimension column (RP) to the second dimension (PGC) was accomplished using a two-position six-port valve inside the column compartment. Following injection onto the RP column, the columns were serially coupled (2.5 min), so that all peaks eluting from the RP column during this time were transferred to the PGC column. The column effluents were combined using a T-connector for introduction to the ESI source [21].

The drying gas was nitrogen with a temperature of 360 °C, the sheath gas temperature was 225 °C, and the sheath gas flow rate was 13 L/min. Other parameters were as follows: nebulizer gas pressure of 30 psi, MS capillary voltage of 3500 V, nozzle voltage of 500 V, and the fragmentor voltage of 275 V. After tuning in the 2-GHz extended dynamic range mode with a mass range of 50–1700 m/z, mass calibration was performed immediately prior to measurements using a supplied tune mixture of the manufacturer as described in previous work [21].

For TOFMS-only operation, spectra were acquired with 3 TOF spectra per second. For standard IM-TOFMS operation, the IM trapping funnel was operated with an accumulation time of 10 000 μs and released packages of ions every 45 ms with a trap release time of 150 μs set within the software. For 4-bit multiplexed IM-TOFMS operation, a trapping time of 1.25 ms was used to yield an equivalent trapping time of 10 ms according to the employed pseudo-random sequence hardcoded for this acquisition mode (000100110101111). Detailed method settings can be found in the ESM.

Post-processing of data

Data files collected using the multiplexing mode were firstly de-multiplexed using vendor-supplied software with no smoothing applied. All LC×IM-TOFMS files could then be post-processed for online accurate mass calibration using the reference masses of calibrant ions (see "HPLC-MS instrumentation"). The $^{DT}CCS_{N2}$ values for the metabolite ions in the positive mode were determined using a single-field calibration function which was obtained via the measurement of a series of calibrant ions with conditional reference $^{DT}CCS_{N2}$ values representing the best estimate of the true values [6].

Data processing

Following post-processing, data files were imported into Skyline (v3.6) with formula annotations of targeted metabolites added to the method [22]. Data for each metabolite was extracted in the software in a targeted fashion using the accurate mass of the primary ion species, $^{DT}CCS_{N2}$, and retention

time for the "transition list" workflow based on the assessment of experimental QC samples. The ion match tolerance was 0.005 Da. Metabolite annotation was supported by results from previous work [6, 20]. Unweighted linear regression was used for all calibration curves in the quantification settings.

Simulation studies

Simulations of ions within the RF field of the trapping funnel were performed using SIMION Version 8.1 with the hard-sphere collision model (collision_hs1.lua) and the Poisson potential array refinement methods. A set of five ion masses was used in the model matching a subset of ion masses from the experimental section of this paper together with a couple of higher mass ions from the standard calibration solution (*m*/*z* 161.1, 272.0, 460.2, 922, and 2722). $^{DT}CCS_{N2}$ values for these ions were taken from measured values [6]. The geometry for the full trapping funnel was used in the model (2D axisymmetric), though ions were modeled starting just past the funnel throat prior to the ion trapping section. Experimentally applied values were used for the RF amplitudes and all DC voltages. To capture effects on the fields and ion motion, a continuous beam of ions from the entrance funnel section was modeled by inserting 16 ions of each mass at each 100 μs time slice to represent the ions entering the funnel trapping region from upstream. Ion charge was recorded every 5 μs into a charge array with a scaling factor that modeled an assumed ion current entering the trap region of 1 nA. At the end of each time slice, the ions that did not strike an electrode were saved to a file and kept internally for use in the next time slice. Subsequent time slices modeled the new ions entering the space and added the ions remaining from the previous time slice, preserving position and velocity. The model continued through a full trap load-release cycle consisting of 4 ms pre-load time, 10 ms load time, and an additional 500 μs release and post-release time so that ions released from the trap could be tracked for a sufficient amount of time representing a full ion mobility cycle. In this way, as the model time progressed, the simulation started with only 80 ions, and by the end of the run had input over 11,000 ions into the model. The actual number of ions remaining at each time step depended on ion losses during the run. Distributions of ion positions at any time step as well as resulting potentials were recorded.

Results and discussion

Assessment of ion trapping funnel performance

The Agilent IM-QTOF instrument (Agilent Technologies, Santa Clara, CA) used in this study allows multiple ion optics settings and trapping conditions to be adjusted as part of tuning procedures within acquisition software. By selection of pre-optimized conditions within the software, the tuning procedure can be directed toward improving the transmission of low molecular mass (and/or fragile) ions by the adjustment of both pre- and post-IM ion optics settings. While this procedure provides extremely robust settings for ion transmission, additional variation of trapping RF and increasing the trap release time can further improve abundances in the low *m*/*z* region.

For initial attempts to assess instrument performance, a set of simple infusion experiments were performed to characterize the trapping behavior of different ion species when operating with the IM-MS acquisition mode. As expected, the abundances of a standardized tune ion mixture across a wide mass range (322–922) were found to follow almost quantitative performance across a broad range of trapping times representing up to 90% of the duty cycle (Fig. 1a). This result is in good agreement with early studies of this trap design [18] and also demonstrates the suitability of tuning procedures used for optimizing transmission across this *m*/*z* range. While this result is pleasing with regard to larger, secondary metabolites and lipid-like species, not shown in this diagram is the lowest mass tune ion (*m*/*z* 118) for which transmission was observed to be far from ideal. With this in mind, further infusion experiments focusing on mixtures of low molecular mass metabolites including primary amino acids and nucleosides were undertaken using an analogous experiment design (Fig. 1b). Despite the optimized tune settings relating to trapping funnel conditions (e.g., confining RF field, trap release time), a strong divergence between the expected and experimental data was observed. For some metabolites (particularly those with *m*/*z* below 250), the abundance was in fact decreased as the trapping times exceeded 50% of the duty cycle. For moderately sized metabolites (e.g., riboflavin), we note that some confounding factors may potentially influence this behavior in the trapping funnel (e.g., competitive ionization, polarizability). Nevertheless, we sought further theoretical insight in order to better understand this experimentally observed discrimination against low molecular mass ions, which was consistent regardless of the molecular class considered.

Trapping funnel simulation studies

The electrodynamic trapping funnel used in the Agilent IM-QTOF instrument utilizes RF electric field on the stacked ring electrodes to radially confine ions while DC voltages on the grids and the ring electrodes create a potential well and trap the ions axially [18]. To better understand the behavior of different ion species in this environment, simulation studies were carried out in a systematic series of time slices representing conventional trapping and release of ions into the drift cell.

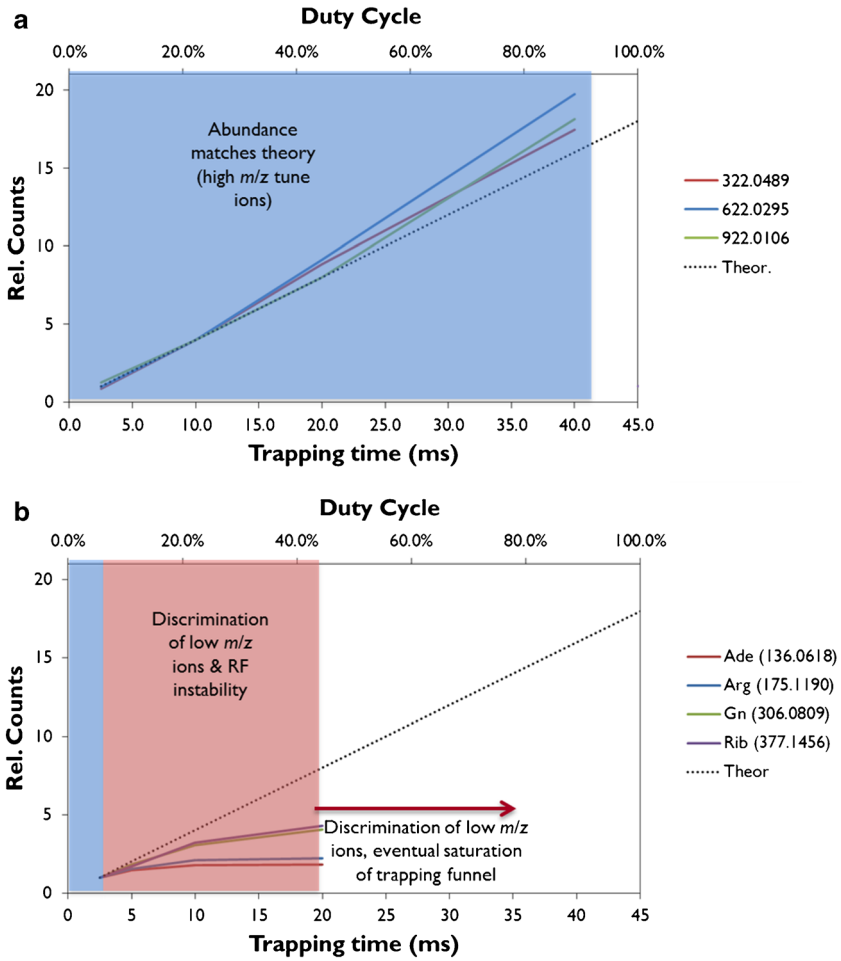

Fig. 1 Results of infusion experiments using standard IM-TOFMS conditions following tuning optimization for small, fragile ions. **a** Results for the most abundant tune ion species present in the manufacturer-supplied mixture. **b** Results from a mixture of four metabolites (all 2.5 μmol/L) using the same experiment design (adenine, arginine, guanosine, riboflavin). Blue shading indicates the region of predictable, quantitative trapping behavior; red shading indicates onset of non-ideal trapping effects for low *m*/*z* ions observed

The trap-release cycle consists of a sequence of voltages applied to an entrance grid and to two exit grids forming the ends of a cylindrical space bounded by the circular RF funnel electrodes. First, ions are kept in the pre-trap area by raising the potential of entrance grid (grid 0). This allows most ions to be lost to the outer RF rings prior to trap loading. For the trap loading time, this trap entrance grid voltage is reduced to a value that allows ions to enter the trap region. During the trapping time, the exit grid voltages (grid 1 and grid 2) are raised to prevent ions from moving forward into the IM section. Initial simulation runs were done to examine effects of space charge in the funnel throat prior to the trapping region. The results show that there were no ion losses although the charge distorts the DC fields in the throat region. Figure 2 illustrates the trap potentials during loading and shows a longitudinal slice through the model with ion positions. Note that the high mass ions are held at distances from the RF ring fields inversely proportional to mass, but this relation breaks down for the lower mass ions (see ESM Annex S3). This occurs since the effective pseudo-potential is reduced more for the low mass ions due to their higher mobility in the same region where the space charge potential counteracts the pseudo-potential. So the lowest mass ions are no longer efficiently trapped by the RF pseudo-potential.

The model shows that once the charge in the trap has accumulated to a few hundred thousand ions, the lowest mass ion reaches a saturation point where those ions are lost at the outer RF ring walls at about the same rate as they enter from the input beam. This appears to be the mechanism behind the experimentally observed low mass sensitivity losses.

The simulation results indicate that space charge from the first ions to accumulate causes later arriving ions to shift further back and toward the rings. The accumulation of charge near the rings creates a DC potential gradient in that location which is countered by the RF pseudo-potential. Although the RF pseudo-potential height is normally inversely proportional to mass, the higher mobility of the low mass ions reduces this value to the point that the lowest mass ions are not held within the trap once sufficient charge has built up (Fig. 3). Eventually, higher *m*/*z* ions also exit to the rings as space charge continues to rise, but this is not experimentally observed to be the case with typical filling times and concentrations. Conversely, for low molecular mass metabolites, low *m*/*z* ions are lost ahead of higher *m*/*z* ions as space charge builds, meaning that the relative metabolite abundance is compromised.

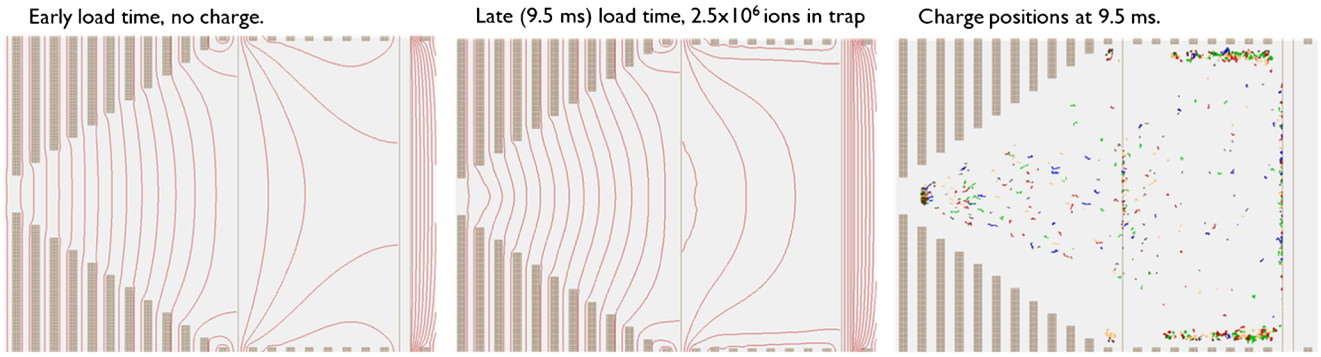

Fig. 2 Equipotential lines in the trapping region during the trap loading time before and after charge have accumulated in the trap. Charge accumulations can be seen near the inside periphery of the ring electrodes before the first grid, in the trap region before the exit grids, and near the inside periphery of the ring electrodes in the funnel trap region. Ions with different *m*/*z* values are held radially at different distances from the inside periphery of the ring electrodes due to mass-dependent pseudo-potential fields, but stay axially within a short distance of the exit grid 1. The stability of the low mass ions under the influence of the applied DC fields, the space charge potentials, and the RF pseudo-potentials causes low mass ions to be preferentially lost to the electrodes once sufficient charge density has built up

Annotation of metabolites: $^{DT}CCS_{N2}$ accuracy

As part of establishing multiplexed IM operation for routine non-targeted metabolomics campaigns, the accuracy of ^{DT}CCS determination was examined using a set of standards previously studied in an interlaboratory study based on this instrument class [6]. Single-field calibration data were collected using the same multiplexed operation settings used for the measurements, and all were de-multiplexed with the same settings. Data collected in standard and multiplexed mode using different ESI source settings to those in [6] were nevertheless found to be in excellent agreement with a maximum difference of 0.2 Å^2 (Table 1). Difference to the established primary stepped field method was larger (average absolute value of 0.61%), but this was in good agreement with previous assessments. This result demonstrates that $^{DT}CCS_{N2}$ values recorded with 4-bit multiplexed operation (^{4}mIM-MS) are fully compatible with values determined by established protocols from standard mode operation (i.e., IM-MS).

Trueness assessment: amino acid CRM

While non-targeted metabolomics relies on differential analysis without the use of independently prepared standards for external calibration, the nature of relative quantification for differential analysis nevertheless depends upon the ability to relate signal intensity to the amount of a metabolite in a sample with sufficient sensitivity. Therefore, an additional confirmation of quantitative capabilities when using multiplexed operation was sought via a trueness test. Measurements of a certified reference material (CRM) and calibration solutions prepared from high-purity standards indicated that the full measurement and data processing workflow did not inhibit accurate quantification with all values determined within the

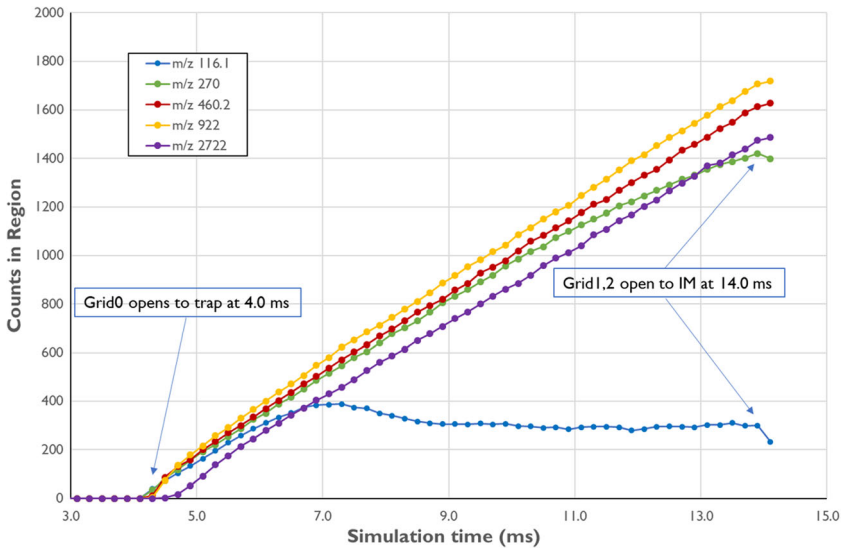

Fig. 3 The number of simulated ions within the trap region is shown for the different masses modeled. The lowest mass reaches a saturation point after about 3 ms into the trap loading time while other masses continue to accumulate in the trap. At the end of the 10-ms loading period, the second lowest *m*/*z* ion is also accumulating in a non-linear manner

Table 1 Comparison of DTIM-MS metabolomics data recorded in standard and multiplexed mode operation with reference values from a previous interlaboratory study. All data were measured in triplicate with repeatability precision of < 0.1% in all examples. Metabolite abbreviations can be found in the ESM (Table S1). [#]Referenced values are from the same instrument from measurements made in 2016

Metabolite	*m/z*	$[M+H]^+$ $^{DT}CCS_{N2}$ (Å^2)			
		Agilent reference (stepped field)	[#]Interlaboratory reference (single field) [6]	Results from this study	
				IM-MS	[4]mIM-MS
P5P	248.0319	151.9	151.3	151.4	151.5
L-Pro	116.0706	126.2	125.1	125.2	125.2
L-Leu	132.1019	135.6	134.6	134.6	134.6
L-i-Leu	132.1019	133.8	132.8	132.9	132.9
L-Met	150.0583	134.1	133.0	133.0	133.0
L-His	156.0768	132.7	131.8	131.8	131.9
L-Phe	166.0863	141.3	140.4	140.3	140.3
L-Arg	175.1190	136.8	136.3	136.3	136.4
L-Tyr	182.0812	146.4	145.7	145.5	145.5

certified range for the CRM (Fig. 4). While absolute quantification of metabolites is not the primary application of LC×IM-TOFMS instrumentation, the maintained accuracy of the result and improvement in sensitivity when using multiplexed operation are important results for extension to measurements of real samples in a non-targeted metabolomics workflow.

Equivalent trapping time condition (standard vs. multiplexed IM operation)

As part of the full measurement campaign, measurements of QC samples were used to ensure that instrumental drift did not inhibit interpretation of experimental results. The QC sample in this experiment was an equimolar mixture of natural metabolites prepared without labeled yeast extract and was measured 3 times for each applied method across the analytical sequence. Repeatability precision (compound abundance) was < 20% RSD for 27 of the 36 metabolites present in the QC sample across the full measurement sequence (see ESM Table S5), which was not surprising given established problems for accurate quantification in metabolomics based on poor retention and/or metabolite stability. For this reason, some metabolites (e.g., serine) were excluded for further assessments so that all acquisition settings could be uniformly compared.

For a comparison of the improvements derived from multiplexed IM experiments, data from an equivalent trapping time experiment (10 ms, or 8 × 1.25 ms for multiplexed measurements) were compared with that from TOF-only measurements. Considering only the IM and [4]mIM-TOFMS measurements, the sensitivity gain factor for metabolites present in the labeled yeast extract was determined by the ratio of the slopes of the internal calibration curves from the respective measurement modes (i.e., natural metabolites spiked in various concentrations into U^{13}C-labeled yeast matrix). In Fig. 5, the correlation of *m/z* with decreasing sensitivity gain factor can be clearly observed as a dramatic improvement is observed with *m/z* values below 250, where up to a 9-fold increase in sensitivity is gained with implementation of 4-bit multiplexing. Across the calibration range studied, we observed a very good linearity for all 27 metabolites with an average R^2 of > 0.992. While not explicitly assessed across all metabolites studied in

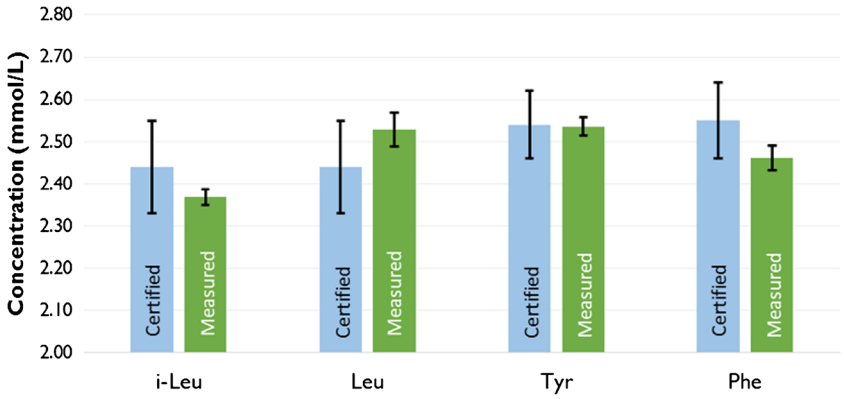

Fig. 4 Comparison of quantitative results for amino acids obtained using multiplexed operation RPLC×IM-TOFMS with certified values for NIST 2389a. Error bars shown for measured data correspond to ±2 s and the error bars for certified values correspond to expanded uncertainties

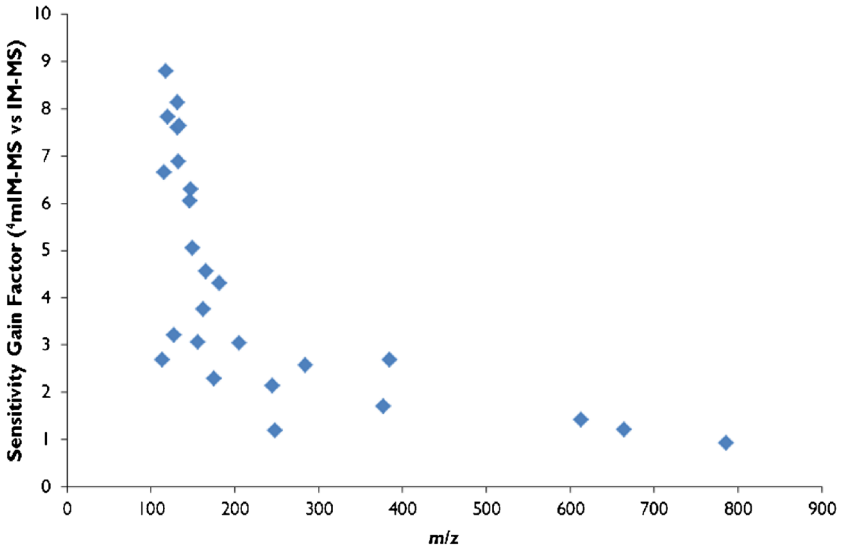

Fig. 5 Experimental sensitivity gain factors (ratio of slope of the calibration curves) determined for 27 metabolites according to the *m/z* of the primary (most abundant) ion species in positive mode based on equivalent trapping times for LC×IM-MS methods

this work, we can estimate that the instrumental dynamic range approaches 4 to 4.5 for small metabolites with the implementation of 4-bit multiplexing due to the combination of improved sensitivity and later onset of TOF detector saturation at high concentrations (in comparison with conventional IM-MS operation). This result underlies the importance of optimization of trapping conditions as part of method development for metabolome assessment using LC×IM-MS.

Of additional interest for emerging analytical method development with IM-MS platforms is the consideration that the combination of pre-concentration of ions in the trapping funnel and the filtering effect of the arrival time distribution can improve detectability of low abundance signals. In order to correctly assess this, method-based limits of quantification and detection (LOQ and LOD) need to be determined according to recognized procedures and also consider repeatability of all data acquisition and processing steps leading to the reported result. To this end, LOQ and LOD values were determined for six metabolites according to EURACHEM Guideline "Fitness for Purpose of Analytical Methods." This approach uses repeated measurements of independently prepared blank or fortified blank samples to yield a standard deviation that is in turn used to estimate these method parameters (Table 2). For all examples studied, the use of the modified Hadamard transform multiplexing provides improved detectability over standard IM-TOFMS operation and even approaches that of LC-TOFMS despite the low (25%) ion utilization efficiency employed in this experiment.

Conclusion

Like all MS-based platforms, analytical method development using IM-MS for metabolomics requires critical assessment of quantitative performance to be considered fit-for-purpose. Evaluation of trapping behavior by simulation and experimental studies demonstrates the need for multiplexed IM-MS operation mode for small metabolites according to improved analytical figures of merit and annotation of low abundance metabolites. The simulation results may also point the way to future improvements in trap design to raise the space–charge-related limits and spur further studies of trapping behavior with different ion populations to better understand other trapping effects not solely determined by *m/z*. Data in this study obtained for 27 diverse metabolites covering a mass range of 90–788 *m/z* demonstrate

Table 2 Results of limit of quantification assessment using full analytical method and data processing workflow

	LC-TOFMS	LC-IM-MS		LC-^{4}mIM-MS	
Metabolite	LOD (μmol/L)	LOD (μmol/L)	Factor loss (vs. TOF)	LOD (μmol/L)	Factor loss (vs. TOF)
Pro	0.14	0.72	5.3	0.19	1.4
Phe	0.14	0.37	2.7	0.12	0.87
Rib	0.23	0.66	2.8	0.26	1.1
Leu	0.035	0.19	5.5	0.055	1.6
SAH	0.016	0.073	4.5	0.025	1.5
Tyr	0.065	0.14	2.1	0.042	0.65

the suitability of DTIM-MS for non-targeted metabolomics in difficult matrices when consideration of trapping conditions is involved in the method development. Based on these results, the combination of the suitable trapping funnel capacity and modified Hadamard multiplexed operation extends effective working range and improves lower working limits of operation for non-targeted metabolomics. Importantly, the accuracy of the key identification parameters derived from IM-TOFMS measurements (single field–derived $^{DT}CCS_{N2}$) is fully maintained with respect to conditional reference standards when employing the multiplexed operation. These results are promising for emerging method development for non-targeted complex sample analysis.

Acknowledgments Vienna Business Agency and EQ BOKU VIBT GmbH are acknowledged for providing mass spectrometry instrumentation.

Compliance with ethical standards

Conflict of interest The authors declare that they have no conflicts of interest.

References

1. May JC, Gant-Branum RL, McLean JA. Targeting the untargeted in molecular phenomics with structurally-selective ion mobility-mass spectrometry. Curr Opin Biotechnol. 2016;39:192–7. https://doi.org/10.1016/j.copbio.2016.04.013.
2. Burnum-Johnson KE, Baker ES, Metz TO. Characterizing the lipid and metabolite changes associated with placental function and pregnancy complications using ion mobility spectrometry-mass spectrometry and mass spectrometry imaging. Placenta. 2017. https://doi.org/10.1016/j.placenta.2017.03.016.
3. Zhang X, Kew K, Reisdorph R, Sartain M, Powell R, Armstrong M, et al. Performance of a high-pressure liquid chromatography-ion mobility-mass spectrometry system for metabolic profiling. Anal Chem. 2017;89:6384–91. https://doi.org/10.1021/acs.analchem.6b04628.
4. Zheng X, Aly NA, Zhou Y, Dupuis KT, Bilbao A, Paurus VL, et al. A structural examination and collision cross section database for over 500 metabolites and xenobiotics using drift tube ion mobility spectrometry. Chem Sci. 2017;8:7724–36. https://doi.org/10.1039/C7SC03464D.
5. Mairinger T, Causon TJ, Hann S. The potential of ion mobility–mass spectrometry for non-targeted metabolomics. Curr Opin Chem Biol. 2018;42:9–15. https://doi.org/10.1016/j.cbpa.2017.10.015.
6. Stow SM, Causon TJ, Zheng X, Kurulugama RT, Mairinger T, May JC, et al. An interlaboratory evaluation of drift tube ion mobility–mass spectrometry collision cross section measurements. Anal Chem. 2017;89:9048–55. https://doi.org/10.1021/acs.analchem.7b01729.
7. Paglia G, Williams JP, Menikarachchi L, Thompson JW, Tyldesley-Worster R, Halldórsson S, et al. Ion mobility derived collision cross sections to support metabolomics applications. Anal Chem. 2014;86:3985–93. https://doi.org/10.1021/ac500405x.
8. Paglia G, Astarita G. Metabolomics and lipidomics using traveling-wave ion mobility mass spectrometry. Nat Protoc. 2017;12:797–813. https://doi.org/10.1038/nprot.2017.013.
9. Righetti L, Bergmann A, Galaverna G, Rolfsson O, Paglia G, Dall'Asta C. Ion mobility-derived collision cross section database: application to mycotoxin analysis. Anal Chim Acta. n.d.. https://doi.org/10.1016/j.aca.2018.01.047.
10. Kyle JE, Casey CP, Stratton KG, Zink EM, Kim Y-M, Zheng X, et al. Comparing identified and statistically significant lipids and polar metabolites in 15-year old serum and dried blood spot samples for longitudinal studies. Rapid Commun Mass Spectrom. 2017;31:447–56. https://doi.org/10.1002/rcm.7808.
11. Zhang X, Romm M, Zheng X, Zink EM, Kim Y-M, Burnum-Johnson KE, et al. SPE-IMS-MS: an automated platform for sub-sixty second surveillance of endogenous metabolites and xenobiotics in biofluids. Clin Mass Spectrom. 2016;2:1–10. https://doi.org/10.1016/j.clinms.2016.11.002.
12. Nichols CM, Dodds JN, Rose B, Picache JA, Morris CB, Codreanu SG, et al. Untargeted molecular discovery in primary metabolism: collision cross section as a molecular descriptor in ion mobility-mass spectrometry. Anal Chem. 2018. https://doi.org/10.1021/acs.analchem.8b04322.
13. Picache JA, Rose BS, Balinski A, Leaptrot KL, Sherrod SD, May JC, et al. Collision cross section compendium to annotate and predict multi-omic compound identities. Chem Sci. 2019. https://doi.org/10.1039/C8SC04396E.
14. Bino RJ, Hall RD, Fiehn O, Kopka J, Saito K, Draper J, et al. Potential of metabolomics as a functional genomics tool. Trends Plant Sci. 2004;9:418–25. https://doi.org/10.1016/j.tplants.2004.07.004.
15. Cajka T, Fiehn O. Toward merging untargeted and targeted methods in mass spectrometry-based metabolomics and lipidomics. Anal Chem. 2016;88:524–45. https://doi.org/10.1021/acs.analchem.5b04491.
16. Ortmayr K, Causon TJ, Hann S, Koellensperger G. Increasing selectivity and coverage in LC-MS based metabolome analysis. TrAC Trends Anal Chem. 2016;82:358–66. https://doi.org/10.1016/j.trac.2016.06.011.
17. Belov ME, Buschbach MA, Prior DC, Tang K, Smith RD. Multiplexed ion mobility spectrometry-orthogonal time-of-flight mass spectrometry. Anal Chem. 2007;79:2451–62. https://doi.org/10.1021/ac0617316.
18. Clowers BH, Ibrahim YM, Prior DC, Danielson WF, Belov ME, Smith RD. Enhanced ion utilization efficiency using an electrodynamic ion funnel trap as an injection mechanism for ion mobility spectrometry. Anal Chem. 2008;80:612–23. https://doi.org/10.1021/ac701648p.
19. Causon T, Kurulugama R, Hann S. Drift-tube ion mobility mass spectrometry for non-targeted 'omics. Methods Mol Biol Submitt. n.d..
20. Ortmayr K, Hann S, Koellensperger G. Complementing reversed-phase selectivity with porous graphitized carbon to increase the metabolome coverage in an on-line two-dimensional LC-MS setup for metabolomics. Analyst. 2015;140:3465–73. https://doi.org/10.1039/c5an00206k.
21. Causon TJ, Ivanova-Petropulos V, Petrusheva D, Bogeva E, Hann S. Fingerprinting of traditionally produced red wines using liquid chromatography combined with drift tube ion mobility-mass spectrometry. Anal Chim Acta. 2019;1052:179–89. https://doi.org/10.1016/j.aca.2018.11.040.
22. MacLean BX, Pratt BS, Egertson JD, MacCoss MJ, Smith RD, Baker ES. Using skyline to analyze data-containing liquid chromatography, ion mobility spectrometry, and mass spectrometry dimensions. J Am Soc Mass Spectrom. 2018;29:2182–8. https://doi.org/10.1007/s13361-018-2028-5.

Tim Causon obtained his PhD in 2012 at the University of Tasmania, Australia, and is now an assistant professor at the University of Natural Resources and Life Sciences in Vienna, Austria. His research interests are focused on MS, ion mobility–MS, and separation science technologies, including fundamental studies and analytical method development for metabolomics and related small molecule applications. He is also an editorial advisory board member of *Analytica Chimica Acta*.

Ruwan T. Kurulugama serves as the senior R&D scientist and project manager for Ion Mobility QTOF instrument development group in Agilent's Mass Spectrometry Division and led the development of Agilent's uniform field IM-QTOF instrument. His current research focus is to develop ion mobility and mass spectrometry–based analytical tools and techniques and ion activation and fragmentation methods. He is also involved in data acquisition and data processing software developments.

Le Si-Hung is a PhD candidate at the Institute of Analytical Chemistry of the University of Natural Resources and Life Sciences, Vienna. He has been working under the supervision of Professor Stephan Hann (BOKU, Vienna) within the topic of analytical method development for non-targeted and targeted metabolomics involving biotechnologically relevant yeast cell extracts since 2016.

John C. Fjeldsted serves as the Senior Director for Ion Mobility and Intellectual Property for Agilent's Mass Spectrometry Division and is an Agilent distinguished scientist. John's nearly 40-year career in spectrometry has covered a very wide range of instrumentation and informatics explorations and development. Of particular interest is the standardization of CCS measurement and using ion mobility enable workflows to support higher confidence in analyte identification.

Ken Newton is a computational physicist and senior R&D scientist at Agilent Technologies in Santa Clara, CA, USA, and has been working in mass spectrometry instrument design for over 15 years. The work has included development of optimization algorithms and new approaches to use of cloud and HPC computing for modeling and designing ion optics and ion source design.

Stephan Hann heads the group of Instrumental Analytical Chemistry and Metabolomics at the University of Natural Resources and Life Sciences, Vienna. The research of his group aims at the development and application of analytical methods in mass spectrometry–based metabolomics and ultra-trace analysis applied to a broad range of research topics.